

Remarkable Luminescence Properties of Lanthanide Complexes with Asymmetric Dodecahedron Structures

Kohei Miyata,^[a] Tetsuya Nakagawa,^[b] Ryuhei Kawakami,^[c] Yuki Kita,^[c] Katsufumi Sugimoto,^[c] Takuya Nakashima,^[b] Takashi Harada,^[b] Tsuyoshi Kawai,^{*,[b]} and Yasuchika Hasegawa^{*,[a]}

Abstract: The distorted coordination structures and luminescence properties of novel lanthanide complexes with oxo-linked bidentate phosphane oxide ligands—4,5-bis(diphenylphosphoryl)-9,9-dimethylxanthene (xantpo), 4,5-bis(di-*tert*-butylphosphoryl)-9,9-dimethylxanthene (*t*Bu-xantpo), and bis[(2-diphenylphosphoryl)phenyl] ether (dpepo)—and low-vibrational frequency hexafluoroacetylacetonato (hfa) ligands are reported. The lanthanide

complexes exhibit characteristic square antiprism and trigonal dodecahedron structures with eight-coordinated oxygen atoms. The luminescence properties of these complexes are characterized by their emission quantum yields, emission lifetimes, and their radiative

Keywords: lanthanides • luminescence • phosphane ligands • samarium • structure elucidation

and nonradiative rate constants. Lanthanide complexes with dodecahedron structures offer markedly high emission quantum yields (Eu: 55–72%, Sm: 2.4–5.0% in [D₆]acetone) due to enhancement of the electric dipole transition and suppression of vibrational relaxation. These remarkable luminescence properties are elucidated in terms of their distorted coordination structures.

Introduction

There has been significant recent interest in the development of luminescent metal complexes for applications that include optical materials,^[1] organic light-emitting diodes (OLEDs),^[2] and fluorescent sensors.^[3] The luminescence properties of transition-metal complexes are derived from the d–d and MLCT (metal-to-ligand charge-transfer) transi-

tions based on the d orbitals of the complexes. These luminescence properties are strongly dominated by the organic ligands and the coordination structure. The designs of organic ligands and coordination structures are directly linked to control of the ligand field. In particular, the ligand field of transition-metal complexes is strongly affected by geometrical structures.^[4] A large number of scientific studies on geometrical structures and luminescence properties of luminescent metal complexes have been reported.^[5]

Here we focus on luminescent lanthanide complexes with 4f orbitals. Lanthanide complexes with characteristic narrow emission bands and long emission lifetimes have been regarded as attractive luminescent materials for use in electroluminescent (EL) devices,^[6] lasers,^[7] and luminescent biosensing applications.^[8] In general, the luminescence properties of lanthanide complexes derived from f–f transitions also depend on their coordination structures. The coordination number of lanthanide ions in solution is known to vary from 8 to 12 depending on the nature of the ligating molecules.^[9] Specific coordination structures give rise to lanthanide complexes with strong and characteristic luminescence properties.^[10–12] The characteristic coordination structures of luminescent lanthanide complexes have been extensively studied.^[13]

[a] K. Miyata, Prof. Dr. Y. Hasegawa
Division of Materials Chemistry, Graduate School of Engineering
Hokkaido University, North-13 West-8, Kita-ku, Sapporo
Hokkaido 060-8628 (Japan)
Fax: (+81)11-706-7114
E-mail: hasegaway@eng.hokudai.ac.jp

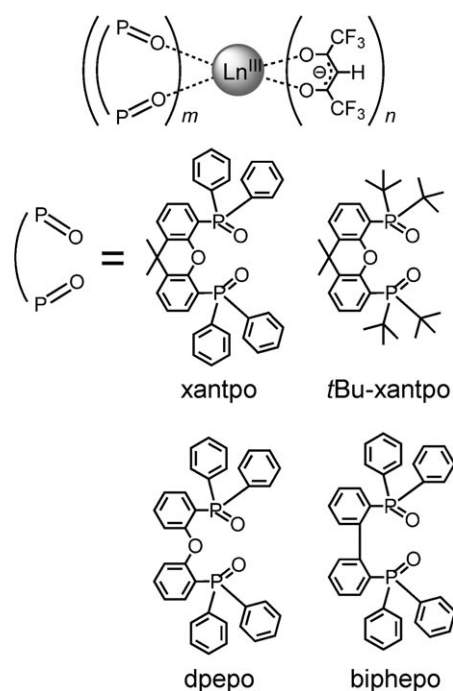
[b] Dr. T. Nakagawa, Assoc.-Prof. Dr. A.-P. D. T. Nakashima, T. Harada,
Prof. Dr. T. Kawai
Graduate School of Materials Science
Nara Institute of Science and Technology
8916-5, Takayama, Ikoma, Nara 630-0192 (Japan)

[c] R. Kawakami, Y. Kita, K. Sugimoto
Nishi-Yamato Gakuen Senior High School
295 Kawai-Cho, Nara 636-0082 (Japan)

Supporting information for this article is available on the WWW under <http://dx.doi.org/10.1002/chem.201001993>. It includes the decay profiles of the lanthanide complexes and the calculations of the S values for the lanthanide complexes.

The characteristic coordination structures and luminescence properties of lanthanide complexes are dominated by the steric and vibrational structures of the organic ligands. In earlier studies, we prepared an Eu^{III} complex with low-vibrational frequency (LVF) hexafluoroacetylacetonato (hfa) and bidentate phosphane oxide ligands, $[\text{Eu}(\text{hfa})_3(\text{biphepo})]$ (biphepo: 1,1'-biphenyl-2,2'-diylbis(diphenylphosphane oxide)).^[14] The coordination structure composed of LVF phosphane oxides ($\text{P}=\text{O}$: 1125 cm^{-1}) and hfa ligands provides the Eu^{III} complex with a high emission quantum yield ($\Phi = 60\%$) and a relatively small nonradiative rate constant. The coordination geometry of $[\text{Eu}(\text{hfa})_3(\text{biphepo})]$ is categorized as a square antiprism (8-SAP) without a symmetry axis. The characteristic 8-SAP structure is composed of three hfa ligands and one biphepo ligand, which leads to a reduction of the geometrical symmetry of the Eu^{III} complex, and consequently $[\text{Eu}(\text{hfa})_3(\text{biphepo})]$ shows a relatively large radiative rate constant. On the other hand, the geometrical symmetry of lanthanide complexes is regarded as a significant factor that influences the transition probabilities. Generally, lanthanide complexes with low-symmetric coordination structures exhibit high-emission quantum yields with large radiative rate constants.^[12] Raymond et al. have proposed a symmetric factor, the shape measure S , to estimate the geometrical distortion of lanthanide complexes.^[15] We have also found that distortion of the coordination structures of Eu^{III} complexes leads to the enhancement of the electric dipole transition probability.^[16] Here, we focus on an oxo-linked bidentate phosphane framework as a novel ligand of a lanthanide complex for enhancement of geometrical distortion. Oxo-linked bidentate phosphane ligands have been known to provide a large bite angle between a metal ion and phosphorus atoms in the metal complex.^[17] We consider that the introduction of an oxo-linked bidentate phosphane framework into coordination sites of lanthanide complexes might lead to expansion of their bite angles related to geometrical distortion. Based on these structural and photophysical findings, a lanthanide complex with distorted coordination structure composed of oxo-linked bidentate phosphane oxide ligands is expected to give rise to an increase in the electric dipole transition probability.

We report here on the characteristic photophysical properties of lanthanide complexes with novel asymmetric structures (trigonal dodecahedron structures) composed of three kinds of oxo-linked bidentate phosphane oxide ligands as shown in Scheme 1 (xantpo: 4,5-bis(diphenylphosphoryl)-9,9-dimethylxanthene; *t*Bu-xantpo: 4,5-bis(di-*tert*-butylphosphoryl)-9,9-dimethylxanthene; dpepo: bis[(2-diphenylphosphoryl)phenyl] ether). Robertson and co-workers have recently reported that an Eu^{III} complex with hfa and dpepo ligands shows strong luminescence properties in polymer thin films;^[13b] however, the geometrical structure and radiative rate constants of lanthanide complexes with dpepo ligands have not yet been reported. We have characterized the geometrical structures of Eu^{III} and Sm^{III} complexes using X-ray single-crystal analyses and shape-measure criteria. The luminescence properties were characterized by their emission



Scheme 1. Chemical structures of lanthanide complexes with bidentate phosphane oxides ($\text{Ln} = \text{Eu}, \text{Sm}$; $m = 1, 2$; $n = 2, 3$).

quantum yields, emission lifetimes, and their radiative and nonradiative rate constants. Based on the structural and photophysical results, the remarkable luminescence properties of lanthanide complexes with dodecahedron structures have been demonstrated for the first time. We also report that the emission quantum yield of $[\text{Sm}(\text{hfa})_3(\text{dpepo})]$ with a trigonal dodecahedron structure is the highest in previously reported Sm^{III} complexes. These remarkable luminescence properties are elucidated in terms of their distorted coordination structures.

Results and Discussion

Coordination structures of lanthanide complexes with oxo-linked bidentate phosphane oxides: Single crystals of lanthanide complexes with oxo-linked bidentate phosphane oxides were successfully prepared for X-ray single-crystal analyses by recrystallization from solutions in methanol. The resulting crystal data are summarized in Tables 1 and 2. The ORTEP views of all the lanthanide complexes show eight-coordinated structures (Figures 1 and 2). The coordination sites of $[\text{Eu}(\text{hfa})_3(\text{tBu-xantpo})]$, $[\text{Eu}(\text{hfa})_3(\text{dpepo})]$, $[\text{Eu}(\text{hfa})_3(\text{biphepo})]$, $[\text{Sm}(\text{hfa})_3(\text{tBu-xantpo})]$, and $[\text{Sm}(\text{hfa})_3(\text{dpepo})]$ comprise three hexafluoroacetylacetonato (hfa) ligands and one bidentate phosphane oxide ligand. In contrast, the coordination sites of $[\text{Eu}(\text{hfa})_2(\text{xantpo})_2]$ and $[\text{Sm}(\text{hfa})_2(\text{xantpo})_2]$ comprise two hfa ligands and two bidentate phosphane oxide ligands with the hexafluoroacetylacetonato anion (hfa^- : $\text{CF}_3\text{COC}^-\text{HCOCF}_3$) and trifluoroacetate anion (CF_3COO^-) counterions, respectively. We have considered

Table 1. Crystal data of Eu^{III} complexes.

	[Eu(hfa) ₂ (xantpo) ₂]	[Eu(hfa) ₃ (tBu-xantpo)]	[Eu(hfa) ₃ (dpepo)]	[Eu(hfa) ₃ (biphepo)] ^[a]
formula	C ₉₃ H ₆₇ F ₁₈ O ₁₂ P ₄ Eu	C ₄₆ H ₅₁ F ₁₈ O ₉ P ₂ Eu	C ₅₁ H ₅₁ F ₁₈ O ₉ P ₂ Eu	C ₅₁ H ₅₁ F ₁₈ O ₈ P ₂ Eu
<i>M_r</i>	1994.37	1303.78	1343.68	1327.68
crystal color, habit	colorless, block	colorless, block	colorless, block	colorless, block
crystal system	triclinic	monoclinic	triclinic	monoclinic
space group	<i>P</i> $\bar{1}$ (no. 2)	<i>P</i> 2 ₁ / <i>c</i> (no. 14)	<i>P</i> $\bar{1}$ (no. 2)	<i>P</i> 2 ₁ / <i>n</i> (no. 14)
<i>a</i> [Å]	12.8434(2)	21.9134(5)	12.3802(5)	13.1819(2)
<i>b</i> [Å]	17.9406(3)	20.1740(5)	13.3535(5)	31.5572(6)
<i>c</i> [Å]	19.2651(4)	24.1073(6)	18.6388(9)	13.5087(3)
α [°]	84.3311(7)		82.4190(13)	
β [°]	82.6768(7)	149.9133(7)	77.2612(15)	111.4181(7)
γ [°]	80.9203(7)		62.3602(9)	
<i>V</i> [Å ³]	4333.60(14)	5342.7(2)	2660.94(19)	5231.31(17)
<i>Z</i>	2	4	2	4
ρ_{calcd} [g cm ⁻³]	1.528	1.621	1.677	1.686
<i>T</i> [°C]	-170 ± 1	-90 ± 1	-90 ± 1	-170 ± 1
μ (MoK α) [cm ⁻¹]	8.967	13.449	13.535	13.745
max 2 θ [°]	55.0	50.6	50.7	55.0
measured reflns	43 429	42 405	21 981	51 911
unique reflns	19 805	9 700	9 698	11 985
<i>R</i> (<i>I</i> > 2 σ (<i>I</i>)) ^[b]	0.0453	0.0287	0.0385	0.0340
<i>R_w</i> (<i>I</i> > 2 σ (<i>I</i>)) ^[c]	0.1366	0.0720	0.1062	0.0910

[a] See ref. [14]. [b] $R = \sum ||F_o| - |F_c|| / \sum |F_o|$. [c] $R_w = [(\sum w(|F_o| - |F_c|)^2) / \sum w F_o^2]^{1/2}$.

Table 2. Crystal data of Sm^{III} complexes.

	[Sm(hfa) ₂ (xantpo) ₂]	[Sm(hfa) ₃ (tBu-xantpo)]	[Sm(hfa) ₃ (dpepo)]
formula	C ₉₃ H ₇₈ F ₁₅ O ₁₅ P ₄ Sm	C ₄₆ H ₅₁ F ₁₈ O ₉ P ₂ Sm	C ₅₁ H ₅₁ F ₁₈ O ₉ P ₂ Sm
<i>M_r</i>	1994.90	1302.22	1342.12
crystal color, habit	colorless, block	colorless, block	colorless, block
crystal system	triclinic	monoclinic	triclinic
space group	<i>P</i> $\bar{1}$ (no. 2)	<i>P</i> 2 ₁ / <i>n</i> (no. 14)	<i>P</i> $\bar{1}$ (no. 2)
<i>a</i> [Å]	12.9433(4)	12.1153(5)	12.3661(5)
<i>b</i> [Å]	17.7795(7)	20.1706(7)	13.4079(6)
<i>c</i> [Å]	19.4357(7)	21.8687(8)	18.5261(7)
α [°]	85.0606(10)		82.2082(12)
β [°]	82.9841(10)	95.0228(12)	77.0833(10)
γ [°]	82.0480(11)		61.9059(11)
<i>V</i> [Å ³]	4385.6(3)	5323.6(3)	2639.56(19)
<i>Z</i>	2	4	2
ρ_{calcd} [g cm ⁻³]	1.511	1.625	1.689
<i>T</i> [°C]	-140 ± 1	-100 ± 1	-150 ± 1
μ (MoK α) [cm ⁻¹]	8.143	12.797	12.939
max 2 θ [°]	50.6	50.6	50.6
measured reflns	35 841	42 569	21 444
unique reflns	15 874	9 688	9 574
<i>R</i> (<i>I</i> > 2 σ (<i>I</i>)) ^[a]	0.0309	0.0287	0.0378
<i>R_w</i> (<i>I</i> > 2 σ (<i>I</i>)) ^[b]	0.0705	0.0984	0.1055

[a] $R = \sum ||F_o| - |F_c|| / \sum |F_o|$. [b] $R_w = [(\sum w(|F_o| - |F_c|)^2) / \sum w F_o^2]^{1/2}$.

that the trifluoroacetate anion in Figure 2 might be formed by the oxidation reaction of the hexafluoroacetylacetonato ligand.^[18]

Based on the crystal data, we carried out the calculations of the shape factor *S* to estimate the degree of distortion of the coordination structure in first coordination sphere.^[15] The *S* value is given by Equation (1):

$$S = \min \sqrt{\left(\frac{1}{m}\right) \sum_{i=1}^m (\delta_i - \theta_i)^2} \quad (1)$$

in which *m*, δ_i and θ_i are the number of possible edges (*m* = 18 in this study), the observed dihedral angle between planes along the *i*th edge and the dihedral angle for the ideal structure, respectively. The estimated *S* values of lanthanide complexes are summarized in Table 3 (see Figures S1–S3 and Tables S1–S8 in the Supporting Information). For [Eu(hfa)₂(xantpo)₂], the *S* value for the eight-coordinated square anti-prism structure (8-SAP, point group: *D*_{4d}, *S* = 3.0°) is smaller than that for the eight-coordinated trigonal dodecahedron structure (8-TDH, point group: *D*_{2d}, *S* = 13°), thereby suggesting that the 8-SAP structure is less distorted than the 8-TDH structure. We thus determined that the coordination geometry of [Eu(hfa)₂(xantpo)₂] is 8-SAP. Based on the minimum value of *S*, the coordination geometries of lanthanide complexes with *t*Bu-xantpo and dpepo ligands are classified as 8-TDH, whereas those with xantpo and biphepo ligands are classified as 8-SAP. These estimations also suggest that the geometrical symmetry in the first coordination sphere of lanthanide complexes with *t*Bu-xantpo and dpepo ligands (point group: *D*_{2d}) is lower than those of lanthanide complexes with xantpo and biphepo ligands (point group: *D*_{4d}).

We also determined the symmetrical point groups of the lanthanide complexes concerned with the locations of phosphane oxide and β -diketonato linker species (Figure 3). The symmetrical point groups of [Eu(hfa)₃(tBu-xantpo)], [Eu(hfa)₃(dpepo)], [Sm(hfa)₃(tBu-xantpo)], and [Sm(hfa)₃(dpepo)] were found to be quasi-*C*₁. On the other hand, those of [Eu(hfa)₂(xantpo)₂] and [Sm(hfa)₂(xantpo)₂] were categorized as quasi-*C*₂ because of their two coordinated xantpo ligands. We have also reported that the coordination structure of [Eu(hfa)₃(biphepo)] was classified as 8-SAP with quasi-*C*₁ symmetry.^[14] These results indicate that lanthanide complexes with 8-TDH geometry (*D*_{2d}) and quasi-*C*₁ symmetry are expected to enhance the electric transition probability in the 4f orbi-

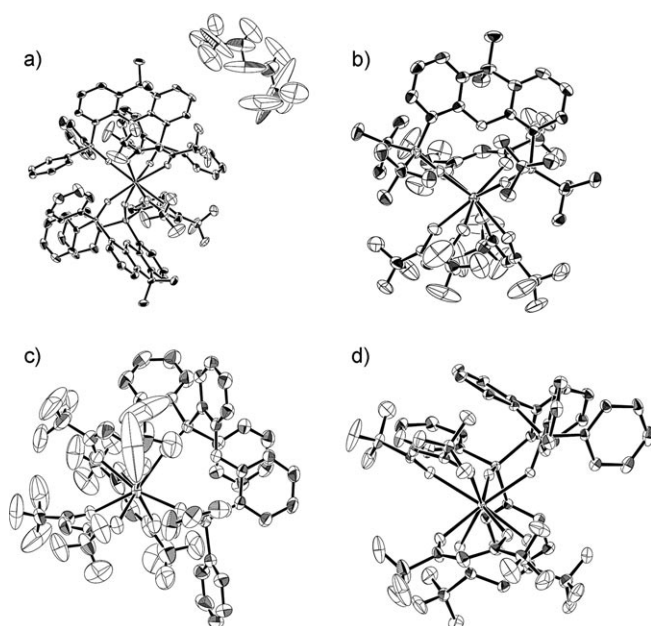


Figure 1. ORTEP drawing of Eu^{III} complexes. Hydrogen atoms have been omitted for clarity and thermal ellipsoids are shown at the 50% probability level.

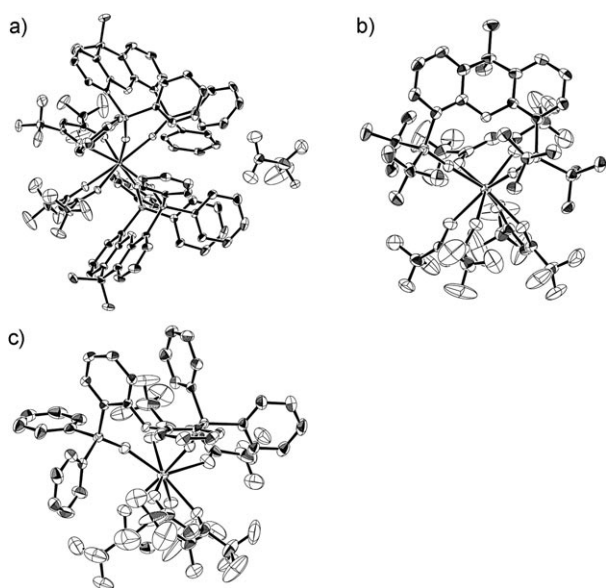


Figure 2. ORTEP drawing of Sm^{III} complexes. Hydrogen atoms have been omitted for clarity and thermal ellipsoids are shown at the 50% probability level.

tals related to the change in odd parity. The characteristic structures of these lanthanide complexes are likely to affect their photophysical properties significantly.

Photophysical properties of eight-coordinated lanthanide complexes: The steady-state emission spectra of lanthanide complexes in $[\text{D}_6]$ acetone are shown in Figure 4. Emission bands of Eu^{III} complexes are observed at around 578, 592, 613, 650, and 698 nm, and are attributed to the f–f transi-

Table 3. Shape-measure calculations of the Eu^{III} and Sm^{III} complexes.^[a]

Complex	$S(D_{2d})^{[b]}$ [°]	$S(D_{4d})^{[c]}$ [°]	Determined co-ordination geometry
$[\text{Eu}(\text{hfa})_2(\text{xantpo})_2]$	13	3.0	8-SAP
$[\text{Eu}(\text{hfa})_3(\text{tBu-xantpo})]$	5.6	13	8-TDH
$[\text{Eu}(\text{hfa})_3(\text{dpepo})]$	4.7	16	8-TDH
$[\text{Eu}(\text{hfa})_3(\text{biphepo})]$	13	3.7	8-SAP
$[\text{Sm}(\text{hfa})_2(\text{xantpo})_2]$	13	2.7	8-SAP
$[\text{Sm}(\text{hfa})_3(\text{tBu-xantpo})]$	5.6	12	8-TDH
$[\text{Sm}(\text{hfa})_3(\text{dpepo})]$	4.4	14	8-TDH

[a] See the Supporting Information. [b] S value for eight-coordinated trigonal dodecahedron (8-TDH). [c] S value for eight-coordinated square antiprism (8-SAP).

tions of ${}^5\text{D}_0\text{--}{}^7\text{F}_J$ with $J=0, 1, 2, 3$, and 4, respectively. Emission bands of Sm^{III} complexes are also observed at around 562, 598, 642 and 704 nm, and are attributed to the f–f transitions of ${}^4\text{G}_{5/2}\text{--}{}^6\text{H}_J$ with $J=5/2, 7/2, <9/2>$, and $11/2$, respectively. The spectra are normalized with respect to the magnetic dipole transition intensities at 592 nm (Eu : ${}^5\text{D}_0\text{--}{}^7\text{F}_1$) and at 598 nm (Sm : ${}^4\text{G}_{5/2}\text{--}{}^6\text{H}_{7/2}$), which are known to be insensitive to the surrounding environment of the lanthanide ions.^[19] The emission bands at 613 nm (Eu : ${}^5\text{D}_0\text{--}{}^7\text{F}_2$) and 642 nm (Sm : ${}^4\text{G}_{7/2}\text{--}{}^6\text{H}_{5/2}$) are due to electric dipole transitions, which are strongly dependent on their coordination geometry. The emission quantum yields for Eu^{III} and Sm^{III} complexes in $[\text{D}_6]$ acetone excited at their 4f orbitals (direct excitation) were found to be 55–72% and 2.4–5.0%, respectively (Table 4). These values are similar to those reported for

Table 4. Photophysical properties of the Eu^{III} and Sm^{III} complexes in $[\text{D}_6]$ acetone at room temperature.

Complex	$\Phi^{[a]}$ [%]	$\tau_{\text{obsd}}^{[b]}$ [ms]	$k_r^{[c]}$ [s^{-1}]	$k_{\text{nr}}^{[d]}$ [s^{-1}]
$[\text{Eu}(\text{hfa})_2(\text{xantpo})_2]$	55	1.3	4.4×10^2	3.6×10^2
$[\text{Eu}(\text{hfa})_3(\text{tBu-xantpo})]$	67	1.2	5.5×10^2	2.7×10^2
$[\text{Eu}(\text{hfa})_3(\text{dpepo})]$	72	1.5	4.7×10^2	1.8×10^2
$[\text{Eu}(\text{hfa})_3(\text{biphepo})]^{[e]}$	60	1.3	4.6×10^2	3.1×10^2
$[\text{Sm}(\text{hfa})_2(\text{xantpo})_2]$	3.8	0.35	1.1×10^2	2.8×10^3
$[\text{Sm}(\text{hfa})_3(\text{tBu-xantpo})]$	2.4	0.15	1.6×10^2	6.5×10^3
$[\text{Sm}(\text{hfa})_3(\text{dpepo})]$	5.0	0.28	1.8×10^2	3.3×10^3

[a] Emission quantum yields for Eu^{III} complexes were determined by comparison with the integrated emission signal (550–750 nm) of $[\text{Eu}(\text{hfa})_3(\text{biphepo})]$ as $\Phi=0.60$. Excitation at 465 nm. Emission quantum yields for Sm^{III} complexes were determined by comparison with the integrated emission signal (550–750 nm) of $[\text{Sm}(\text{hfa})_3(\text{H}_2\text{O})_2]$ as $\Phi=0.031$. Excitation at 481 nm. [b] Emission lifetime (τ_{obsd}) of the lanthanide complexes were measured by excitation at 355 nm (Nd:YAG 3 ω). [c] Radiative rate constants $k_r = \Phi/\tau_{\text{obsd}}$. [d] Nonradiative rate constants $k_{\text{nr}} = 1/\tau_{\text{obsd}} - k_r$. [e] See ref. [20].

$[\text{Eu}(\text{hfa})_3(\text{tppo})_2]$ ($\Phi=65\%$; tppo: triphenylphosphine oxide) and $[\text{Sm}(\text{hfa})_3(\text{tppo})_2]$ ($\Phi=4.1\%$) in $[\text{D}_6]$ acetone, which have been reported to be highly luminescent lanthanide complexes.^[20,21] To the best of our knowledge, the emission quantum yield for $[\text{Sm}(\text{hfa})_3(\text{dpepo})]$ ($\Phi=5.0\%$) is the highest of previously reported Sm^{III} complexes.

The time-resolved emission profiles of lanthanide complexes revealed single-exponential decays with lifetimes on

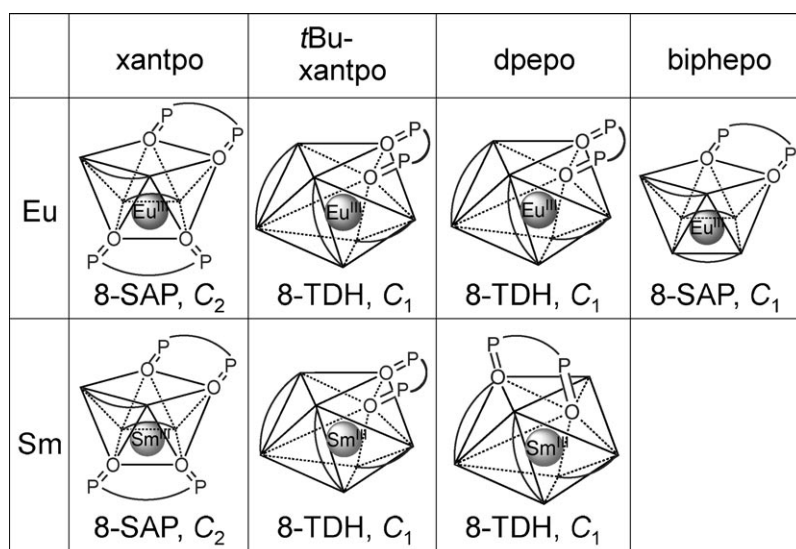


Figure 3. Geometrical coordination structure images of Eu^{III} and Sm^{III} complexes. Coordinated oxygen atoms are shown as corner polyhedra. Curved lines between oxygen atoms represent phosphane oxide and hfa ligands.

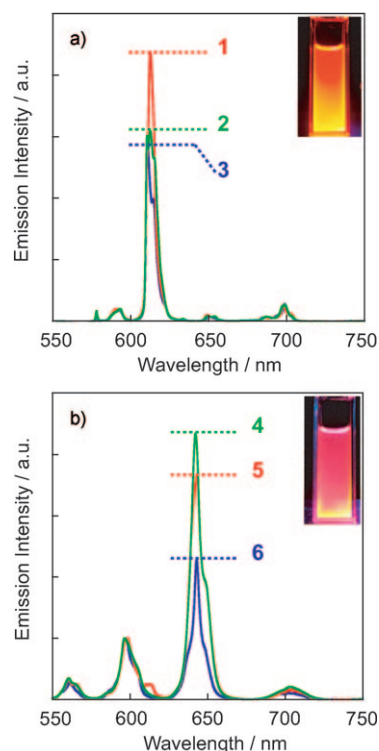


Figure 4. a) Emission spectra of [Eu(hfa)₃(*t*Bu-xantpo)] (red line 1), [Eu(hfa)₃(dpepo)] (green line 2), and [Eu(hfa)₂(xantpo)₂] (blue line 3) in [D₆]acetone at room temperature. Excited at 465 nm. The spectra were normalized with respect to the magnetic dipole transition (⁵D₀–⁷F₁). b) Emission spectra of [Sm(hfa)₃(dpepo)] (green line 4), [Sm(hfa)₃(*t*Bu-xantpo)] (red line 5), and [Sm(hfa)₂(xantpo)₂] (blue line 6) in [D₆]acetone at room temperature. Excited at 402 nm. The spectra were normalized with respect to the magnetic dipole transition (⁴G_{7/2}–⁶H_{7/2}).

the millisecond timescale (see Figures S4 and S5 in the Supporting Information). The emission lifetimes were determined from the slopes of logarithmic plots of the decay profiles. The radiative (k_r) and nonradiative (k_{nr}) rate constants estimated by using the emission lifetimes and the emission quantum yields are summarized in Table 4. The k_r values for [Eu(hfa)₃(*t*Bu-xantpo)] and [Eu(hfa)₃(dpepo)] were found to be 5.5×10^2 and 4.7×10^2 s⁻¹, respectively. These k_r values are larger than that for [Eu(hfa)₂(xantpo)₂] (4.4×10^2 s⁻¹). We also observed that the k_r values for [Sm(hfa)₃(*t*Bu-xantpo)] and [Sm(hfa)₃(dpepo)] are larger than that for [Sm(hfa)₂(xantpo)₂]. In general, reduction

of the geometrical symmetry of the coordination structure leads to a larger k_r value.^[22] We suggest that k_r for lanthanide complexes with phosphane oxides depends on the symmetry of the coordination sites.

From Table 4, it can also be seen that k_{nr} for [Sm(hfa)₃(*t*Bu-xantpo)] is much larger than the values for the other lanthanide complexes. Note that the energy gap of the Sm^{III} ion is smaller than that of the Eu^{III} ion (Sm^{III}: 7500 cm⁻¹, Eu^{III}: 12500 cm⁻¹). The excited state of the Sm^{III} ion with a smaller energy gap is effectively quenched by vibrational relaxation of the high-vibrational-frequency C–H bonds. We have considered that the larger k_{nr} values for [Sm(hfa)₃(*t*Bu-xantpo)] might be attributed to effective vibrational relaxation caused by the thirty-six C–H bonds in the four *tert*-butyl groups attached to the phosphorus atoms.

We thus conclude that the symmetry of coordination structures of lanthanide complexes is correlated to their photophysical properties. To produce strong luminescence in luminescent lanthanide complexes, the following intrinsic requirements should be fulfilled: 1) low-vibrational structure, 2) an asymmetrical point group (8-TDH), and 3) asymmetrical coordination structures (quasi-C₁).

Conclusion

We have successfully synthesized novel lanthanide complexes that contain oxo-linked bidentate phosphane oxide ligands xantpo, *t*Bu-xantpo, and dpepo with high emission quantum yields. They exhibited characteristic luminescence properties depending on their coordination structures. Recently, the effects on the Ln–X polarizations have also been reported.^[23] Here we have demonstrated characteristic photophysical properties for eight-coordinated lanthanide com-

plexes with trigonal dodecahedron structures for the first time. Such strongly luminescent lanthanide complexes with distorted coordination structures would open up new fields in photophysical, coordination, and material chemistry.

Experimental Section

Materials: Europium acetate monohydrate (99.9%), samarium acetate tetrahydrate (99.9%), [D₆]acetone (D, 99.9%), and CDCl₃ (D, 99.8%) were purchased from Wako Pure Chemical Industries Ltd. 1,1,1,5,5,5-Hexafluoro-2,4-pentanedione, 4,5-bis(diphenylphosphino)-9,9-dimethylxanthene, 4,5-bis(di-*tert*-butylphosphino)-9,9-dimethylxanthene, and bis[(2-diphenylphosphino)phenyl] ether were obtained from Tokyo Kasei Organic Chemicals and Aldrich Chemical Company Inc. All other chemicals and solvents were reagent grade and were used without further purification.

Apparatus: Infrared spectra were recorded using a JASCO FT/IR-420 spectrometer. ¹H (300 and 500 MHz) and ³¹P NMR (200 MHz) spectra were recorded using a JEOL ECP-500. Chemical shifts are reported in δ (ppm) and are referenced to an internal tetramethylsilane standard for ¹H NMR spectroscopy and an external 85% H₃PO₄ standard for ³¹P NMR spectroscopy. Mass spectra were measured using a JEOL JMS-700M Station. Elemental analyses were performed using a Perkin-Elmer 2400II instrument.

Preparation of [Eu(hfa)₃(H₂O)₂]: Europium acetate monohydrate (5.0 g, 13 mmol) was dissolved in distilled water (20 mL) in a 100 mL flask. A solution of 1,1,1,5,5,5-hexafluoro-2,4-pentanedione (7.0 g, 34 mmol) was added dropwise to the solution. The reaction mixture produced a precipitation of white yellow powder after stirring for 3 h at room temperature. The reaction mixture was filtered, and the resulting powder was recrystallized from methanol/water to afford colorless needle crystals of the title compound. Yield: 9.6 g (95%); IR (KBr): $\tilde{\nu}$ = 1650 (st, C=O), 1145–1258 cm⁻¹ (st, C–F); elemental analysis calcd (%) for C₁₅H₇EuF₁₈O₈ (809.91): C 22.48, H 0.88; found: C 22.12, H 1.01.

Preparation of [Sm(hfa)₃(H₂O)₂]: Samarium acetate tetrahydrate (5.0 g, 13 mmol) was dissolved in distilled water (60 mL) in a 100 mL flask. A solution of 1,1,1,5,5,5-hexafluoro-2,4-pentanedione (10 g, 48 mmol) was added dropwise to the solution. The reaction mixture produced a precipitation of white yellow powder after stirring for 1 h at room temperature. The reaction mixture was filtered, and the resulting powder was recrystallized from methanol to afford colorless needle crystals of the title compound. Yield: 8.3 g (82%); IR (ATR): $\tilde{\nu}$ = 3425 (st, O–H), 1646 (st, C=O), 1094–1251 cm⁻¹ (st, C–F); elemental analysis calcd (%) for C₁₅H₇SmF₁₈O₈ (808.91): C 22.31, H 0.87; found: C 21.92, H 1.10.

Preparation of xantpo: 4,5-Bis(diphenylphosphino)-9,9-dimethylxanthene (1.0 g, 1.7 mmol) was dissolved in dichloromethane (20 mL) in a 100 mL flask. The solution was cooled to 0°C, and then a 30% H₂O₂ aqueous solution (4.0 mL, 35 mmol) was added. The reaction mixture was stirred at 0°C for 4 h and was then washed with water and extracted three times with dichloromethane. The organic layer was dried over anhydrous magnesium sulfate and concentrated to dryness. Recrystallization from hexane gave a white powder of the title compound. Yield: 1.1 g (99%); ¹H NMR (300 MHz, CDCl₃, 25°C): δ = 7.58–7.60 (d, *J* = 6 Hz, 2H; Ar), 7.30–7.47 (m, 2H; Ar), 6.94–7.00 (t, *J* = 6 Hz, 2H; Ar), 6.78–6.85 (m, 2H; Ar), 1.69 ppm (s, 6H; 2Me); ³¹P NMR (200 MHz, CDCl₃, 25°C): δ = 33.55 (1P), 30.32 ppm (1P); IR (ATR): $\tilde{\nu}$ = 1190 (st, P=O), 1100–1229 cm⁻¹ (st, C–O–C); FAB-MS: *m/z*: 611 [M+H]⁺.

Preparation of *t*Bu-xantpo: 4,5-Bis(di-*tert*-butylphosphino)-9,9-dimethylxanthene (1.0 g, 2.0 mmol) was dissolved in dichloromethane (20 mL) in a 100 mL flask. The solution was cooled to 0°C, and then a 30% H₂O₂ aqueous solution (4.5 mL, 40 mmol) was added. The reaction mixture was stirred at 0°C for 4 h and was then washed with water and extracted three times with dichloromethane. The organic layer was dried over anhydrous magnesium sulfate and concentrated to dryness. Recrystallization from hexane gave a white powder of the title compound. Yield: 0.97 g

(91%); ¹H NMR (300 MHz, CDCl₃, 25°C): δ = 7.82–7.84 (d, *J* = 6 Hz, 2H; Ar), 7.53–7.60 (m, 2H; Ar), 7.40–7.46 (m, 2H; Ar), 1.67 (s, 6H; 2Me), 1.35–1.46 ppm (m, 36H; 4*t*Bu); ³¹P NMR (200 MHz, CDCl₃, 25°C): δ = 69.53 (1P), 58.36 (1P) ppm; IR (ATR): $\tilde{\nu}$ = 1180 (st, P=O), 1103–1200 cm⁻¹ (st, C–O–C); FAB-MS: *m/z*: 531 [M+H]⁺.

Preparation of dpepo: Bis[(2-diphenylphosphino)phenyl] ether (5.0 g, 9.3 mmol) was dissolved in dichloromethane (100 mL) in a 300 mL flask. The solution was cooled to 0°C, and then a 30% H₂O₂ aqueous solution (21 mL, 186 mmol) was added. The reaction mixture was stirred at 0°C for 4 h and was then washed with water and extracted three times with dichloromethane. The organic layer was dried over anhydrous magnesium sulfate and concentrated to dryness. Recrystallization from hexane gave a white powder of the title compound. Yield: 5.0 g (94%); ¹H NMR (300 MHz, CDCl₃, 25°C): δ = 7.06–7.71 (m, 26H; Ar), 6.02–6.07 ppm (m, 2H; Ar); ³¹P NMR (200 MHz, CDCl₃, 25°C): δ = 26.41 (2P) ppm; IR (ATR): $\tilde{\nu}$ = 1183 (st, P=O), 1070–1226 cm⁻¹ (st, C–O–C); FAB-MS: *m/z*: 571 [M+H]⁺.

General procedure for the preparation of Eu^{III} and Sm^{III} complexes: Phosphane oxide ligand (1 equiv) and [Ln(hfa)₃(H₂O)₂] (1.2 equiv) were dissolved in methanol (30 mL). The solution was heated at reflux while stirring for 8 h, and the reaction mixture was concentrated to dryness. The residue was washed with chloroform several times. The insoluble material was removed by filtration, and the filtrate was concentrated. The obtained powder was dissolved in hot methanol solution (50°C, ca. 1 mL), and was then permitted to stand at room temperature. Recrystallization from methanol gave colorless block crystals of the lanthanide complexes.

Complex [Eu(hfa)₂(xantpo)₂]: Yield: 0.32 g (49%); ¹H NMR (300 MHz, CDCl₃, 25°C): δ = 6.74–7.65 (m), 1.88 ppm (s; Me); ³¹P NMR (200 MHz, [D₆]acetone, 25°C): δ = –92.12 (2P), –98.86 ppm (2P); IR (ATR): $\tilde{\nu}$ = 1653 (st, C=O), 1137 (st, P=O), 1095–1251 cm⁻¹ (st, C–O–C and st, C–F); ESI-MS: *m/z*: calcd for C₈₈H₆₆EuF₁₂O₁₀P₄ [M–(hfa)]⁺: 1787.264; found: 1787.264; elemental analysis calcd (%) for C₉₃H₆₉EuF₁₈O₁₂P₄·1.5 CHCl₃ (1994.25): C 52.22, H 3.18; found: C 52.11, H 3.25.

Complex [Sm(hfa)₂(xantpo)₂]: Yield: 0.79 g (46%); ¹H NMR (500 MHz, [D₆]acetone, 25°C): δ = 5.81–8.09 (m), 1.67 (s; Me), 1.52 ppm (s; Me); ³¹P NMR (200 MHz, [D₆]acetone, 25°C): δ = 33.03 (2P), 32.80 ppm (2P); IR (ATR): $\tilde{\nu}$ = 1653 (st, C=O), 1138 (st, P=O), 1100–1252 cm⁻¹ (st, C–O–C and st, C–F); ESI-MS: *m/z*: calcd for C₈₈H₆₆SmF₁₂O₁₀P₄ [M–(hfa)]⁺: 1786.257; found: 1786.261; elemental analysis calcd (%) for C₉₃H₇₈SmF₁₈O₁₅P₄ (1995.33): C 55.99, H 3.94; found: C 55.54, H 3.53.

Complex [Eu(hfa)₃(*t*Bu-xantpo)]: Yield: 0.35 g (66%); ¹H NMR (300 MHz, CDCl₃, 25°C): δ = 7.41 (m, 2H; Ar), 7.07 (m, 2H; Ar), 6.83 (m, 2H; Ar), 5.92 (s, 3H; hfa-H), 2.97–3.02 (m, 6H; 2Me), 1.41–1.68 ppm (m, 36H; 4*t*Bu); ³¹P NMR (200 MHz, [D₆]acetone, 25°C): δ = 68.41 ppm (2P); IR (ATR): $\tilde{\nu}$ = 1653 (st, C=O), 1138 (st, P=O), 1098–1249 cm⁻¹ (st, C–O–C and st, C–F); ESI-MS: *m/z*: calcd for C₄₁H₃₉EuF₁₂O₇P₂ [M–(hfa)]⁺: 1097.206; found: 1097.206; elemental analysis calcd (%) for C₄₆H₅₁EuF₁₈O₉P₂ (1304.19): C 42.38, H 3.94; found: C 42.93, H 4.00.

Complex [Sm(hfa)₃(*t*Bu-xantpo)]: Yield: 0.39 g (53%); ¹H NMR (500 MHz, [D₆]acetone, 25°C): δ = 8.06–8.08 (d, *J* = 7.5 Hz, 2H; Ar), 7.73–7.77 (m, 2H; Ar), 7.50–7.53 (t, *J* = 7.5 Hz, 2H; Ar), 6.73 (s, 3H; hfa-H), 1.83 (s, 6H; 2Me), 0.52–0.55 ppm (d, *J* = 15 Hz, 36H; 4*t*Bu); ³¹P NMR (200 MHz, [D₆]acetone, 25°C): δ = 62.37 ppm (2P); IR (ATR): $\tilde{\nu}$ = 1653 (st, C=O), 1137 (st, P=O), 1100–1252 cm⁻¹ (st, C–O–C and st, C–F); ESI-MS: *m/z*: calcd for C₄₁H₅₀SmF₁₂O₇P₂ [M–(hfa)]⁺: 1096.204; found: 1096.200; elemental analysis calcd (%) for C₄₆H₅₁SmF₁₈O₉P₂ (1303.19): C 42.43, H 3.95; found: C 42.68, H 3.71.

Complex [Eu(hfa)₃(dpepo)]: Yield: 0.62 g (74%); ¹H NMR (500 MHz, [D₆]acetone, 25°C): δ = 7.32–7.64 (m, 22H; Ar), 7.10–7.13 (t, *J* = 7.5 Hz, 2H; Ar), 6.90–6.95 (dd, *J* = 7.5 Hz, 2H; Ar), 6.73 (s, 3H; hfa-H), 6.29–6.30 ppm (m, 2H; Ar); ³¹P NMR (200 MHz, [D₆]acetone, 25°C): δ = –113.42 ppm (2P); IR (ATR): $\tilde{\nu}$ = 1653 (st, C=O), 1135 (st, P=O), 1098–1251 cm⁻¹ (st, C–O–C and st, C–F); ESI-MS: *m/z*: calcd for C₄₆H₃₀EuF₁₂O₇P₂ [M–(hfa)]⁺: 1137.049; found: 1137.049; elemental analysis calcd (%) for C₅₁H₃₁EuF₁₈O₉P₂ (1344.04): C 45.59, H 2.33; found: C 45.76, H 2.11.

Complex [Sm(hfa)₃(dpepo)]: Yield: 0.66 g (79%); ¹H NMR (500 MHz, [D₆]acetone, 25 °C): δ = 7.32–7.64 (m, 2H; Ar), 7.10–7.13 (t, J = 7.5 Hz, 2H; Ar), 6.90–6.95 (dd, J = 7.5 Hz, 2H; Ar), 6.73 (s, 3H; hfa-H), 6.29–6.30 ppm (m, 2H; Ar); ³¹P NMR (200 MHz, [D₆]acetone, 25 °C): δ = 29.17 ppm (2P); IR (ATR): $\tilde{\nu}$ = 1653 (st, C=O), 1134 (st, P=O), 1098–1250 cm⁻¹ (st, C-O-C and st, C-F); ESI-MS: *m/z*: calcd for C₄₆H₃₀SmF₁₂O₇P₂ [*M*-(hfa)]⁺: 1136.048; found: 1136.044; elemental analysis calcd (%) for C₅₁H₃₁SmF₁₈O₉P₂ (1343.04): C 45.64, H 2.33; found: C 45.54, H 2.18.

Crystallography: Colorless single crystals of lanthanide complexes obtained from the solutions in methanol were mounted on a glass fiber by using epoxy resin glue. All measurements were made using a Rigaku RAXIS RAPID imaging plate area detector with graphite-monochromated MoK α radiation. Corrections for decay and Lorentz-polarization effects were made using empirical absorption correction, solved by direct methods, and expanded using Fourier techniques. Non-hydrogen atoms were refined anisotropically. Hydrogen atoms were refined using the riding model. The final cycle of full-matrix least-squares refinement was based on observed reflections and variable parameters. All calculations were performed using the crystal-structure crystallographic software package. We confirmed the CIF data by using the checkCIF/PLATON service. CCDC-768471 ([Eu(hfa)₂(xantpo)₂]), 768472 ([Eu(hfa)₃(tBu-xantpo)]), 768473 ([Eu(hfa)₃(dpepo)]), 768474 ([Sm(hfa)₂(xantpo)₂]), 768475 ([Sm(hfa)₃(tBu-xantpo)]), and 768476 ([Sm(hfa)₃(dpepo)]) contain the supplementary crystallographic data for this paper. These data can be obtained free of charge from The Cambridge Crystallographic Data Center via www.ccdc.cam.ac.uk/data_request/cif.

Optical measurements: UV/Vis absorption spectra were recorded using a JASCO V-660 spectrometer. Emission spectra of the lanthanide complexes were measured using a Hitachi F-4500 spectrometer and corrected for the response of the detector system. The emission quantum yields of the lanthanide complex solutions degassed with argon (10 mm in [D₆]acetone) were obtained by comparison with the integrated emission signal (550–750 nm) of [Eu(hfa)₃(biphepo)] as a reference (Φ = 0.60: 50 mm in [D₆]acetone) with an excitation wavelength of 465 nm (direct excitation of Eu^{III} ions) for Eu^{III} complexes^[20] or [Sm(hfa)₃(H₂O)₂] as a reference (Φ = 0.031: 100 mm in [D₆]DMSO) with an excitation wavelength of 481 nm (direct excitation of Sm^{III} ions) for Sm^{III} complexes. Emission lifetimes of lanthanide complexes (10 mm in [D₆]acetone) were measured using the third harmonics (355 nm) of a Q-switched Nd:YAG laser (Spectra Physics, INDI-50, fwhm = 5 ns, λ = 1064 nm) and a photomultiplier (Hamamatsu photonics, R5108, response time \leq 1.1 ns). The Nd:YAG laser response was monitored using a digital oscilloscope (Sony Tektronix, TDS3052, 500 MHz) synchronized to the single-pulse excitation. Emission lifetimes were determined from the slope of logarithmic plots of the decay profiles. High-resolution spectra of the emission were measured using a HORIBA SPEX FluoroLog.

Acknowledgements

We thank S. Katao, F. Asanoma, Y. Nishikawa, and M. Yamamura in NAIST for X-ray crystallographic analyses, elemental analyses, NMR spectroscopic, and mass spectroscopic measurements. This work was supported by a Grant-in-Aid for Scientific Research on the Priority Area “Strong Photo-Molecule Coupling Fields for Chemical Reactions,” “Scientific Research on Innovative Areas,” and the Global COE Program (project no. B01: Catalysis as the Basis for Innovation in Materials Science) from the Ministry of Education, Culture, Sports, Science, and Technology (MEXT), Japan.

- [1] a) G. Blasse, B. C. Grabmaier, *Luminescent Materials*; Springer, New York, **1994**; b) A. Vogler, H. Kunkely, *Luminescent Metal Complex: Diversity of Excited States in Transition Metal and Rare Earth Compounds*, Springer, New York, **2001**.
[2] a) R. Gao, D. G. Ho, B. Hernandez, M. Selke, D. Murphy, P. I. Djurovich, M. E. Thompson, *J. Am. Chem. Soc.* **2002**, *124*, 14828–14829;

- b) J. Li, P. I. Djurovich, B. D. Alleyne, M. Yousufuddin, N. N. Ho, J. C. Thomas, J. C. Peters, R. Bau, M. E. Thompson, *Inorg. Chem.* **2005**, *44*, 1713–1727; c) X.-M. Yu, G.-J. Zhou, C.-S. Lam, W.-Y. Wong, X.-L. Zhu, J.-X. Sun, M. Wong, H.-S. Kwok, *J. Organomet. Chem.* **2008**, *693*, 1518.
[3] a) B. K. Kaletas, R. M. Williams, B. Konig, L. De Cola, *Chem. Commun.* **2002**, 776–777; b) S. S. Sun, A. J. Lees, P. Y. Zavalij, *Inorg. Chem.* **2003**, *42*, 3445–3453.
[4] O. Horvath, K. L. Stevenson, *Charge Transfer Photochemistry of Coordination Compound*, VHC, Weinheim, **1992**.
[5] a) V. W.-W. Yam, C. C. Ko, N. Zhu, *J. Am. Chem. Soc.* **2004**, *126*, 12734–12735; b) C. Goze, C. Sabatini, A. Barbieri, F. Barigelletti, R. Ziessel, *Inorg. Chem.* **2007**, *46*, 7341–7350; c) F. Guyon, A. Hameau, A. Khatyr, H. Amrouche, D. Fortin, P. D. Harvey, C. Strohmann, A. L. Ndiaye, V. Huch, M. Veith, N. Avarvari, *Inorg. Chem.* **2008**, *47*, 7483–7492; d) C. J. Adams, N. Fey, Z. A. Harrison, I. V. Sazanovich, M. Towrie, J. A. Weinstein, *Inorg. Chem.* **2008**, *47*, 8242–8257; e) Y. Yamamoto, S. Sawa, Y. Funada, T. Morimoto, M. Falkenstrom, H. Miyasaka, S. Shishido, T. Ozeki, K. Koike, O. Ishitani, *J. Am. Chem. Soc.* **2008**, *130*, 14659–14674; f) M. Kato, Y. Shishido, Y. Ishida, S. Kishi, *Chem. Lett.* **2008**, *37*, 16–17; g) K. Matsumoto, N. Matsumoto, A. Ishii, T. Tsukuda, M. Hasegawa, T. Tsunomura, *Dalton Trans.* **2009**, 6795–6801.
[6] a) T. Jüstel, H. Nikol, C. Ronda, *Angew. Chem.* **1998**, *110*, 3250–3271; *Angew. Chem. Int. Ed.* **1998**, *37*, 3084–3103; b) J. Kido, Y. Okamoto, *Chem. Rev.* **2002**, *102*, 2357–2368; c) J. Yu, L. Zhou, H. Zhang, Y. Zheng, H. Li, R. Deng, Z. Peng, Z. Li, *Inorg. Chem.* **2005**, *44*, 1611–1618; d) H. Xu, K. Yin, W. Huang, *J. Phys. Chem. C* **2010**, *114*, 1674–1683.
[7] a) K. Kuriki, Y. Koike, Y. Okamoto, *Chem. Rev.* **2002**, *102*, 2347–2356; b) Y. Hasegawa, Y. Wada, S. Yanagida, *J. Photochem. Photobiol. C* **2004**, *5*, 183–202.
[8] a) N. Weibel, L. J. Charbonniere, M. Guardigli, A. Roda, R. Ziessel, *J. Am. Chem. Soc.* **2004**, *126*, 4888–4896; b) J.-C. G. Bünzli, C. Piguet, *Chem. Soc. Rev.* **2005**, *34*, 1048–1077; c) S. Faulkner, B. P. Burton-Pye, *Chem. Commun.* **2005**, 259–261; d) J. Yu, D. Parker, R. Pal, R. A. Poole, M. J. Cann, *J. Am. Chem. Soc.* **2006**, *128*, 2294–2299; e) B. McMahon, P. Mauer, C. P. McCoy, T. C. Lee, T. Gunnlaugsson, *J. Am. Chem. Soc.* **2009**, *131*, 17542–17543.
[9] V. S. Sastri, J.-C. G. Bünzli, V. R. Rao, G. V. S. Rayudu, J. R. Perumareddi in *Modern Aspects of Rare Earth and Their Complexes*, Elsevier, New York, **2003**.
[10] K. Lunstroff, P. Nockemann, K. V. Hecke, L. V. Meervelt, C. Görlker-Walrand, K. Binne-mans, K. Driesen, *Inorg. Chem.* **2009**, *48*, 3018–3026.
[11] S. Petoud, S. M. Cohen, J.-C. G. Bünzli, K. N. Raymond, *J. Am. Chem. Soc.* **2003**, *125*, 13324–13325.
[12] Y. Hasegawa, S. Tsuruoka, T. Yoshida, H. Kawai, T. Kawai, *J. Phys. Chem. A* **2008**, *112*, 803–807.
[13] Recent selected papers of luminescent lanthanide complexes: a) A. P. Bassett, S. W. Magennis, P. B. Glover, D. J. Lewis, N. Spencer, S. Parsons, R. M. Williams, L. De Cola, Z. Pikramenou, *J. Am. Chem. Soc.* **2004**, *126*, 9413–9424; b) C. Yang, L. M. Fu, Y. Wang, J. P. Zhang, W. T. Wong, X. C. Ai, Y. F. Qiao, B. S. Zou, L. L. Gui, *Angew. Chem.* **2004**, *116*, 5120–5123; *Angew. Chem. Int. Ed.* **2004**, *43*, 5010–5013; c) P. Lenaerts, K. Driesen, R. Van Deun, K. Binne-mans, *Chem. Mater.* **2005**, *17*, 2148–2154; d) B. D. Chandler, D. T. Cramb, G. K. H. Shimizu, *J. Am. Chem. Soc.* **2006**, *128*, 10403–10412; e) L. J. Charbonniere, N. Hildebrandt, R. F. Ziessel, H. Löchmannsroben, *J. Am. Chem. Soc.* **2006**, *128*, 12800–12809; f) R. Pal, D. Parker, *Chem. Commun.* **2007**, 474–476; g) Y. G. Huang, B. L. Wu, D. Q. Yuan, Y. Q. Xu, F. L. Jiang, M. C. Hong, *Inorg. Chem.* **2007**, *46*, 1171–1176; h) G. S. Kottas, M. Mehlstäubl, R. Fröhlich, L. De Cola, *Eur. J. Inorg. Chem.* **2007**, 3465–3467; i) S. Petoud, G. Muller, E. G. Moore, J. Xu, J. Sokolnicki, J. P. Riehl, U. N. Le, S. M. Cohen, K. N. Raymond, *J. Am. Chem. Soc.* **2007**, *129*, 77–83; j) J. P. Leonard, P. Jensen, T. McCabe, J. E. O’Brien, R. D. Peacock, P. E. Kruger, T. Gunnlaugsson, *J. Am. Chem. Soc.* **2007**, *129*, 10986–10987; k) A. De Bettencourt-Dias, S. Viswanathan, A. Rollett, J.

- Am. Chem. Soc.* **2007**, *129*, 15436–15437; l) X. Y. Chen, X. Yang, B. J. Holliday, *J. Am. Chem. Soc.* **2008**, *130*, 1546–1547; m) E. G. Moore, J. Xu, C. J. Jocher, I. Castro-Rodriguez, K. N. Raymond, *Inorg. Chem.* **2008**, *47*, 3105–3118; n) O. Moudam, B. C. Rowan, M. Alamiry, P. Richardson, B. S. Richards, A. C. Jones, N. Robertson, *Chem. Commun.* **2009**, 6649–6651; o) M. Osawa, M. Hoshino, T. Wada, F. Hayashi, S. Osanai, *J. Phys. Chem. A* **2009**, *113*, 10895–10902; p) D. P. Li, C. H. Li, J. Wang, L. C. Kang, T. Wu, Y. Z. Li, X. Z. You, *Eur. J. Inorg. Chem.* **2009**, 4844–4849; q) N. M. Shavaleev, S. V. Eliseeva, R. Scopelliti, J. C. G. Bünzli, *Chem. Eur. J.* **2009**, *15*, 10790–10802; r) G. E. Kiefer, M. Woods, *Inorg. Chem.* **2009**, *48*, 11767–11778; s) K. A. White, D. A. Chengelis, K. A. Gogick, J. Stehman, N. L. Rosi, S. Petoud, *J. Am. Chem. Soc.* **2009**, *131*, 18069–18071; t) D. B. A. Raj, S. Biju, M. L. P. Reddy, *Dalton Trans.* **2009**, 7519–7528; u) M.-H. Ha-Thi, J. A. Delaire, V. Michelet, I. Leray, *J. Phys. Chem. A* **2010**, *114*, 3264–3269.
- [14] K. Nakamura, Y. Hasegawa, H. Kawai, N. Yasuda, N. Kanehisa, Y. Kai, T. Nagamura, S. Yanagida, Y. Wada, *J. Phys. Chem. A* **2007**, *111*, 3029–3037.
- [15] J. Xu, E. Radkov, M. Ziegler, K. N. Raymond, *Inorg. Chem.* **2000**, *39*, 4156–4164.
- [16] T. Harada, Y. Nakano, M. Fujiki, M. Naito, T. Kawai, Y. Hasegawa, *Inorg. Chem.* **2009**, *48*, 11242–11250.
- [17] P. W. N. M. van Leeuwen, P. C. J. Kamer, J. N. H. Reek, P. Dierkes, *Chem. Rev.* **2000**, *100*, 2741–2769.
- [18] D. A. Johnson, A. B. Waugh, T. W. Hambley, J. C. Taylor, *J. Fluorine Chem.* **1985**, *27*, 371–378.
- [19] a) C. Görller-Walrand, L. Fluyt, A. Ceulemans, W. T. Carnall, *J. Chem. Phys.* **1991**, *95*, 3099–3106; b) M. H. V. Werts, R. T. F. Jukes, J. W. Verhoeven, *Phys. Chem. Chem. Phys.* **2002**, *4*, 1542–1548.
- [20] K. Nakamura, Y. Hasegawa, H. Kawai, N. Yasuda, Y. Tsukahara, Y. Wada, *Thin Solid Films* **2008**, *516*, 2376–2381.
- [21] H. Kawai, C. Zhao, S. Tsuruoka, T. Yoshida, Y. Hasegawa, T. Kawai, *J. Alloys Compd.* **2009**, *488*, 612–614.
- [22] Y. Hasegawa, T. Nakagawa, T. Kawai, *Coord. Chem. Rev.* **2010**, *254*, 2643–2651.
- [23] a) K. Norton, G. A. Kumar, J. L. Dilks, T. J. Emge, R. E. Riman, M. G. Brik, J. G. Brennan, *Inorg. Chem.* **2009**, *48*, 3573–3580; b) K. Binnemans, *Chem. Rev.* **2009**, *109*, 4283–4374.

Received: July 15, 2010
Published online: November 5, 2010